Ain Shams Engineering Journal 16 (2025) 103432

Contents lists available at ScienceDirect

Ain Shams Engineering Journal

journal homepage: www.sciencedirect.com

Full Length Article

Nonlinear convective heat transfer in Maxwell nanofluids with quadratic thermal stratification over a Magnetized inclined Surface: Applications towards engineering Industry

Abbas Khan [a,*], Hashim [a], Muhammad Farooq [a], Wasim Jamshed [b,c,d], Basim M. Makhdoum [e], Nor Ain Azeany Mohd Nasir [f,g]

[a] Department of Mathematics & Statistics, University of Haripur, Haripur 22620 KP, Pakistan
[b] Department of Mathematics, Capital University of Science & Technology (CUST), 44000 Islamabad, Pakistan
[c] College of Engineering, Al-Ayen Iraqi University, An Nasiriyah 64001, Iraq
[d] Department of Computer Engineering, Biruni University, Topkapi Istanbul, Turkey
[e] Mechanical Engineering Department, College of Engineering and Architecture, Umm Al-Qura University, P. O. Box 5555, Makkah 21955, Saudi Arabia
[f] Department of Mathematics Centre for Defence Foundation Studies, Universiti Pertahanan Nasional Malaysia, Kem Sungai Besi, 57000 Kuala Lumpur, Malaysia
[g] Institute for Mathematical Research Laboratory of Computational Sciences and Mathematical Physics, Universiti Putra Malaysia, 43400 UPM Serdang, Selangor, Malaysia

ARTICLE INFO

Keywords:
Inclined surface
Maxwell nanofluid
Quadratic mixed convection
Quadratic thermal stratification
Convective boundary condition
Numerical results

ABSTRACT

This work studies nonlinear mixed convection and nonlinear stratification effects in Maxwell nanofluid flow over an inclined stretching sheet. This research has widespread uses in the fields of medicine, paper and pulp, polymer processing, nuclear power plants, solar collectors, and electronic cooling. The characteristics of heat transfer for Iron oxide (Fe_3O_4) nanoparticles dispersed in base fluid blood and silicone oil are the main focus of the investigation. Due to Fe_3O_4 being photo-catalytic, the nanofluid improves its thermal characteristics, which makes it valuable in medical applications. Radiative heat flux, convective boundary conditions, an inclined magnetic field and quadratic mixed convection effects are included in this analysis. Higher-order ODEs are obtained from governing equations, and the ND Solve method is used to solve them numerically. The results are validated by comparing them with previous research and exhibit good agreement. Important factors that affect temperature and velocity profiles are Deborah number, Lorentz force, thermal Grashof number, and thermal Biot number, which are demonstrated visually. According to the findings, heat transfer increases with rising thermal Biot number and decreases with stronger thermal stratification, whereas the Lorentz force reduces fluid velocity. The findings demonstrate improved material performance and efficiency by using stratified Maxwell nanofluids with quadratic convection models to enhance industrial operations. This knowledge is vital for designing and optimising medical therapies and devices, as it is necessary to maintain the ideal temperature during blood circulation procedures. This analysis is critical to ensure patient safety and treatment effectiveness, particularly in medical operations where mixed convection is crucial in blood circulation.

1. Introduction

Fluids' heat transfer and flow characteristics are ideal for heat carrier applications across diverse industries. Due to water's limited thermal conductivity, significant quantities are required to cool heated objects adequately. The low thermal conductivity of the material results in inefficient heat transfer, necessitating increased energy input and higher operational costs. Therefore, designing a new heat carrier with rapid heat conductivity was necessary. This motivation leads to the establishment of the concept of nanofluid. Nanofluid is known for high heat conductivity and can meet this industrial demand. Nanofluid can be created by suspending nanoparticles into fluid based. Metals, carbides, or oxides are frequently utilized as materials for the nanoparticles in the suspension. Meanwhile, ethylene glycol, water, blood, oil, and kerosene are examples of based fluids. Several mathematicians and physicists have addressed the heat transmission characteristics of nanofluids in this

* Corresponding author.
E-mail address: abbaskhaan0400@gmail.com (A. Khan).

https://doi.org/10.1016/j.asej.2025.103432
Received 11 December 2024; Received in revised form 9 April 2025; Accepted 19 April 2025
Available online 24 April 2025

perspective. Mohammadpour et al. [1] explored the thermal performance of nanofluid flow in a micro-channel heat sink operational with numerous artificial aircraft. Khan et al. [2] explored the influence of Lorentz forces on nanofluid flow past a stretched sheet under radiative conditions. Jamil et al. [3] employed fractional derivatives to study the magnetohydrodynamic flow of Maxwell nanofluids, while Hayat et al. [4] extended this approach to explore the thermal behavior of second grade nanofluids. Anwar and Rasheed [5,6] investigated the heat transferal of nanofluids in fractional inertial flow between non-isothermal boundaries under the influence of magnetic fields at the nanoscale. Anwar [7] further explored heat transference in the existence of magnetic fields and Joule heating using the Cattaneo-Maxwell model. Abundant findings have also focused on the mass and heat transport of nanofluids flowing past finned surfaces, as evidenced by Refs. [8–10]. Awais et al. [11] observed the effect of a stretched surface-induced slippage on magnetohydrodynamics (MHD) nanofluid flow. A few insightful articles on nanofluids flow with magnetic nanoparticles can be found in [12–15].

The nanofluids are used in many industrial fields, including food processing, electronics cooling, automobile cooling systems, medicines, solar reactors, and solar cells. Nanofluids, particularly those enhanced with magnetic nanoparticles, have become indispensable. These fluids, which have blood or silicone oil as their base fluids, have excellent thermal conductivity and are, therefore, very useful in applications where good heat transmission is required. However, the problem of chemical instability has come to light due to their extensive use. In order to solve this, chemically stable nanoparticles, like nickel ferrite or iron oxide, are included in nanofluids to improve their thermal performance while maintaining the fluid's stability. This combination improves the performance of heat transferal in industries where accuracy and dependability are essential by producing a more durable, thermally efficient solution. Ahmad et al. [16] investigated the thermal properties of mixed nanofluid movement composed of nickel-zinc ferrite ($NiZnFe_2O_4$) and Manganese zinc ferrite ($MnZnFe_2O_4$). Mizan et al. [17] investigated the two-layer structure in MHD nanofluid flow around an extended cylinder. In an open chamber, Rajarathinam et al. [18] investigated buoyancy and Marangoni-driven convection in a CNT-water nanofluid, examining the impact of an isothermal solid block and a magnetic field on heat transmission. Sarma et al. [19] analyzed the influence of an inclined magnetic field on bioconvective Casson nanofluid flow with gyrotactic effects over a bidirectional extending sheet. Aljohani et al. [20] considered the effects of convective conditions, magneto-peristaltic flow, mixed convection, and non-Darcy resistance on nanofluid flow.

Furthermore, linear mixed convection is only applicable in some manufacturing and solar industries because of the substantial temperature changed between the appliance's surfaces. In this instance, it makes more sense to consider quadratic mixed convection rather than linear mixed convection. The substantial impact of nonlinearities on flow and thermal transport necessitates their inclusion in the modelling of various phenomena, including combustion, electronic device cooling, solar energy systems, and nuclear reactor protection. Hussain et al. [21] studied the stream of Jeffrey fluid past an extending cylinder with a heat source, employing the non-Fourier heat flux model. Irfan et al. [22] extended their investigation of Carreau nanofluid mass transfer to include convective boundary conditions. Hussain et al. [23] examined the influence of mixed convection on water-based nanofluid flow with carbon nanotubes. Jha and Sarki [24] analyzed the effect of Soret and Dufour effects on velocity in both linear and nonlinear convection scenarios. Rajeev and Mahanthesh [25] explored the significance of quadratic mixed convection on multilayer hybrid nanofluid flow. Kouz et al. [26] observed that quadratic convection leads to decreased temperatures and significantly increased velocities. The oscillatory behavior and amplitude of thermal and magnetic boundary layer flow across a circular heated cylinder with heat source/sink effects were examined by Khedher et al. [27]. Their study brought to light the effects of thermal fluctuations and magnetic intensity on flow stability and heat transmission properties. Ullah and colleagues [28] investigated the effects of Soret/Dufour effects and thermal radiation on the oscillatory behavior and amplitude of Darcian mixed convective heat and mass transfer in nanofluid flow across a porous plate. Jha et al. [29] investigated nonlinear mixed convection in a porous vertical plate under convective boundary conditions. Regression analysis was used by Shaheen et al. [30] to assess the effects of thermal radiation and heat source/sink on the flow and heat transfer properties of a hybrid nanofluid along a vertical stretched cylinder. Taking into account the impact of thermal radiation on heat transfer behavior, Shaheen et al. [31] inspected the hydrothermal characteristics and entropy production impacts of a hybrid nanofluid over a stretching/shrinking sheet. In a computational study of the impacts of entropy generation and thermal radiation in hybrid nanofluid flow across a stretching/shrinking sheet, Naqvi et al. [32] observed energy efficiency and heat transfer properties. Superfluous relevant investigations and applications are unambiguously defined in Ref. [33–37].

Stratification is a crucial phenomenon that results from temperature, concentration, or fluid density changes and affect both natural and industrial processes. Double stratification simultaneous mass and heat transfer improves industrial operations like thermal management, chemical separation, and material testing. When it comes to medical therapies that require temperature-controlled environments, like targeted hyperthermia for cancer therapy, stratification is essential because accurate thermal regulation is essential. In drug delivery systems, stratification is essential for achieving the best possible dispersion and concentration of medicinal drugs. Stratified systems in food processing regulate temperature strata during pasteurization, heating, and cooling to help preserve quality. Moreover, stratification shows a critical task in environmental engineering as it facilitates the optimization of solar ponds and water treatment systems, impacts the behaviour of pollutants, and boosts energy efficiency. These many uses highlight the significance of stratification in the progression of medical treatments, industrial innovations, and sustainable energy solutions. Geetha et al. [38] investigated the flow of MHD fluid towards an exponentially permeable stretched sheet in a thermally and chemically stratified porous medium with a heat source. They found that increasing porosity, suction, and thermal stratification led to decreased velocity and temperature profiles. Srinivasacharya and Surender [39] analyzed mixed convection in a non-Darcy porous medium over a vertical surface. Mutuku and Makinde [40] examined the impact of dual stratification on unsteady MHD nanofluid movement past a horizontal sheet. Reddy Chetteti and Srivastav [41] studied double stratification effects in Newtonian fluid flow over an inclined permeable extended sheet. Mallawi et al. [42] studied the response of dual stratification on the convective movement of a non-Newtonian fluid over a Riga plate, considering Cattaneo-Christov double-flux and radiation effects. Bilal et al. [43] analyzed MHD Williamson fluid movement towards a stretched cylinder with variable thermal conductivity. Numerous studies (Refs. [44–52]) have investigated the impact of nonlinearities on diverse flow models, utilizing a variety of assumptions.

This paper investigates the non-Newtonian flow of Maxwell fluid induced by an inclined stretched surface. It is driven by the widespread incidence of mixed convection flow in lots industrial and engineering processes and by realizing the crucial role played by nonlinear stratified nanofluids in addressing high-temperature challenges. With an emphasis on nonlinear mixed convection and nonlinear thermal stratification in the presence of nanofluids, the study offers insightful information about the applicability of these concepts in industrial systems and enhanced thermal management. The study's main objective is to examine the combined influences on the flow field of nonlinear mixed convection and nonlinear thermal stratification, as well as the connections between these phenomena. To the best of our knowledge, research has yet to be done on this issue. In contemporary research, nonlinearity is recognized as a significant influence on convective flow. Quadratic

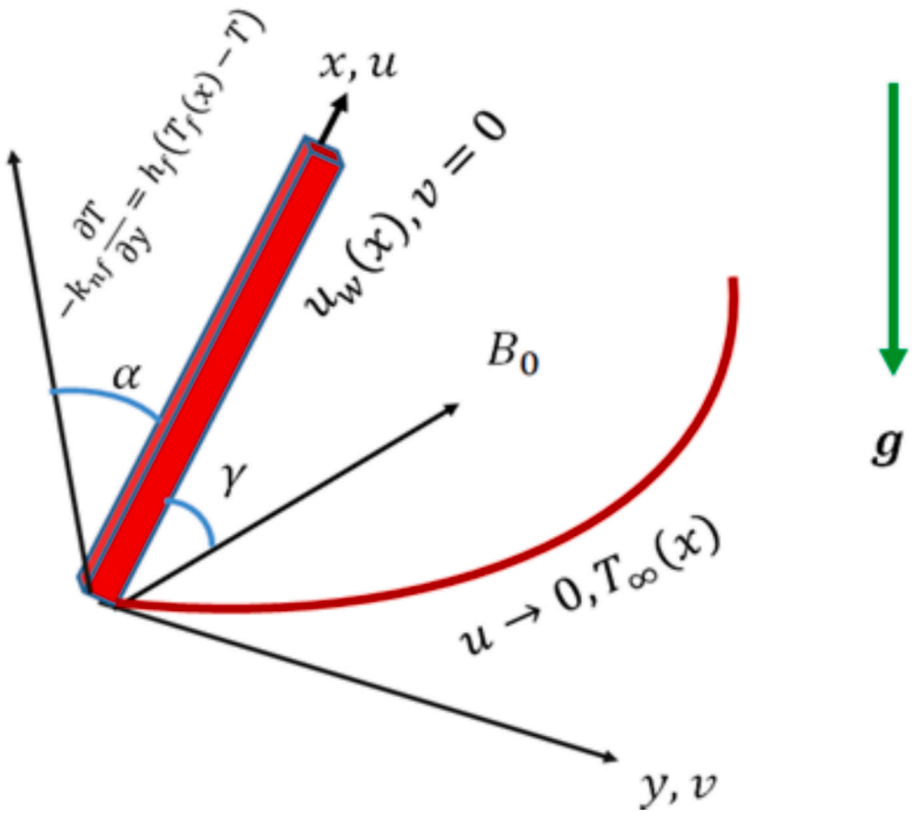

Fig. 1. Physical representation of model problem.

Table 1
Highlights the thermo-physical properties of base fluids and nanoparticles [53].

Thermo-physical Properties	Base fluid		Nanoparticle
	(silicone oil)	Blood	(Fe_3O_4)
$\rho(kg/m^3)$	900	1.050	5200
$c_p(J/kgK)$	1600	3.618	670
$k(W/mK)$	0.15	0.51	6
$\sigma\left(S/m\right)$	1×10^{-8}	0.012	2500
Pr	6.8	21	–

mixed convection of non-Newtonian fluids over linearly stretching inclined sheets has wide-ranging applications in various industries, inclusive of chemical processing, food production, polymer manufacturing, propulsion systems, gas turbines, electronic cooling, and nuclear power. This study focuses on non-Newtonian fluid flow towards a linearly inclined stretched surface, incorporating nonlinear mixed convection, convective boundary conditions, inclined MHD, and nonlinear thermal stratification effects. Similarity transformations are applied to convert the governing PDEs into dimensionless nonlinear ODEs. The velocity and temperature profiles are numerically solved and visualized to understand the influence of key physical parameters. This research is constructed by: Section 2 represents the problem formulation and the subsequent transformation of the governing PDEs into dimensionless nonlinear ODEs. Section 3 outlines the numerical scheme employed. The results and discussion are detailed in Section 4, ended by the resolving statements in Section 5.

2. Physical model formulation

Consider the steady-state incompressible flow of nonlinear mixed convection with nonlinear thermal stratification of a non-Newtonian nanofluid flow induced by a linear inclined stretching surface, where y is the coordinate axis that is normal to the surface and x is the coordinate axis that extends along the surface. It is assumed that u and v represent the $x-$ and $y-$ components of velocity, respectively. The non-Newtonian rate-type behaviour of the fluid is modelled using the Maxwell fluid model. The $u_w(x)$ denotes the stretching velocity with a is a positive constant. The flow is heated convectively at its lower surface, with a temperature T_f and a heat transfer coefficient h_f. In addition to this, a magnetic field with an angle γ in an inclined direction is assumed to be applied to the surface. Thermal radiation is taken into account when analyzing heat transfer. Iron oxide nanoparticles are suspended in silicone oil or blood to create a uniform solution of nanofluid. The aforementioned hypothesis's physical interpretation is shown in Fig. 1. The thermo-physical properties of the nanofluids are provided in Table. 1.

2.1. Momentum equation for Maxwell model

The constitutive equation for Maxwell fluid is

$$\boldsymbol{T} = -P\boldsymbol{I} + \boldsymbol{S} \tag{1}$$

where the symbol $\boldsymbol{T}$ is the Cauchy stress tensor and the extra stress tensor $\boldsymbol{S}$ satisfies

$$\boldsymbol{S} + \lambda_1\left(\frac{d\boldsymbol{S}}{dt} - \boldsymbol{L}\boldsymbol{S} - \boldsymbol{L}^T\boldsymbol{S}\right) = \mu\boldsymbol{A}_1 \tag{12}$$

In which μ is dynamic viscosity, λ_1 is the relaxation time and A_1 is the Rivilin Erickson tensor defined as

$$\boldsymbol{A}_1 = \nabla\boldsymbol{V} + (\nabla\boldsymbol{V})^T \tag{3}$$

For the steady two dimensional flow the equation of momentum for the Maxwell fluid are:

$$\rho\left(u\frac{\partial u}{\partial x}+v\frac{\partial u}{\partial y}\right)=-\frac{\partial P}{\partial x}+\frac{\partial S_{xx}}{\partial x}+\frac{\partial S_{xy}}{\partial y} \tag{4}$$

$$\rho\left(u\frac{\partial v}{\partial x}+v\frac{\partial v}{\partial y}\right)=-\frac{\partial P}{\partial x}+\frac{\partial S_{yx}}{\partial x}+\frac{\partial S_{yy}}{\partial y} \tag{5}$$

Where ρ is fluid density and S_{xx}, S_{xy}, S_{yx} and S_{yy} are components of extra stress tensor. Using the boundary layer approximations:

$$u=O(1), v=O(\delta), x=O(1), y=O(\delta) \tag{6}$$

$$\frac{T_{xx}}{\rho}=O(1), \frac{T_{xy}}{\rho}=O(\delta), \frac{T_{yy}}{\rho}=O\left(\delta^2\right)$$

The flow in the absence of the pressure gradient the Maxwell model momentum equation is of the form

$$u\frac{\partial u}{\partial x}+v\frac{\partial u}{\partial y}+\lambda_1\left(u^2\frac{\partial^2 u}{\partial x^2}+v^2\frac{\partial^2 u}{\partial y^2}+2uv\frac{\partial^2 u}{\partial x\partial y}\right)=v\frac{\partial^2 u}{\partial y^2} \tag{7}$$

Where δ being the boundary layer thickness.

The problem's governing equations for continuity, momentum, and temperature are presented in [54–56], which are then converted to a 2-dimensional nanofluid using the Maxwell fluid model. The boundary layer calculations consider radiation heat flux and the effects of convective boundary conditions. The derived form of the governing continuity, momentum, and energy equations [50] and [51], respectively, are provided as

$$\frac{\partial u}{\partial x}+\frac{\partial v}{\partial y}=0 \tag{8}$$

$$\begin{aligned}&u\frac{\partial u}{\partial x}+v\frac{\partial u}{\partial y}+\lambda_1\left(v^2\frac{\partial^2 u}{\partial y^2}+2uv\frac{\partial^2 u}{\partial x\partial y}+u^2\frac{\partial^2 u}{\partial y^2}\right)-\nu_{nf}\frac{\partial^2 u}{\partial y^2}\\&=g\left[\beta_1(T-T_\infty)+\beta_2(T-T_\infty)^2\right]Cos(\alpha)-\frac{\sigma_{nf}B_0^2}{\rho_{nf}}Sin^2(\gamma)\left(\lambda_1 v\frac{\partial u}{\partial y}+u\right),\end{aligned} \tag{9}$$

$$u\frac{\partial T}{\partial x}+v\frac{\partial T}{\partial y}=\alpha_{nf}\left(\frac{\partial^2 T}{\partial y^2}\right)+\frac{16\sigma^* T_\infty^3}{3K^*(\rho Cp)_f}\left(\frac{\partial^2 T}{\partial y^2}\right). \tag{10}$$

With the associated boundary conditions [35,57] which are as follows:

$$v=0, u=u_w(x), k_{nf}\left(\frac{\partial T}{\partial y}\right)_{y=0}=-h_f\left(T_f(x)-T\right), \text{when} y=0$$

$$u\to 0, T\to T_\infty(x), \text{as} y\to\infty \tag{11}$$

where,

$$u_w(x)=ax, T_f(x)=T_0+a_1x^2, T_\infty(x)=T_0+a_2x^2. \tag{12}$$

It is noted that λ_1 represent the fluid relaxation time, g is the acceleration due to gravity, β_1 signifies the coefficients of thermal linear and β_2 the nonlinear expansions. Meanwhile, K represents the coefficient of thermal conductivity, $T_f(x)$ represents temperature of suspended fluid with the surface temperature and T_∞ is the ambient temperature with $T_\infty > T_\infty$. Other parameters which are σ^* denotes Stefan Boltzmann constant, K^* signifies the mean absorption coefficient, T embodies fluid temperature, T_0 represents reference temperature and d, d_1, α, γ are the dimensional constants, $\alpha_{nf}=\frac{k_{nf}}{(\rho cp)_{nf}}$ denotes the thermal diffusivity of the fluid,cp is heat capacitance, ρ_{nf} symbolizes the effective density, ν_{nf} signifies the kinematic viscosity, k_{nf} denotes effective thermal conductivity σ_{nf}, μ_{nf} the effective viscosity, φ is volume fraction of nanoparticle, and $(\rho cp)_{nf}$ effective heat capacity of nanofluid. The nanofluid parameters are defined as:

$$\mu_{nf}=\frac{\mu_f}{(1-\varphi)^{2.5}} \tag{13}$$

$$\rho_{nf}=(1-\varphi)\rho_f+\varphi\rho_s \tag{14}$$

$$(\rho cp)_{nf}=(1-\varphi)(\rho cp)_f+\varphi(\rho cp)_s \tag{15}$$

$$\sigma_{nf}=\sigma_f\left(1+\frac{3\left(\frac{\sigma_s}{\sigma_f}-1\right)\varphi}{\left(\frac{\sigma_s}{\sigma_f}+2\right)-\left(\frac{\sigma_s}{\sigma_f}-1\right)\varphi}\right) \tag{16}$$

$$\left.\frac{k_{nf}}{k_f}=\frac{k_s+2k_f-2\varphi(k_f-k_s)}{k_s+2k_f+2\varphi(k_f-k_s)}\right\} \tag{17}$$

Take into consideration the following similarity variables:

$$u=axf'(\eta), v=-\sqrt{av_f}f(\eta), \theta(\eta)=\frac{T-T_\infty}{T_f-T_0}, \eta=y\sqrt{\frac{a}{v_f}} \tag{18}$$

and utilizing the concept of stream functions,

$$u=\frac{\partial\psi}{\partial y}=axf'(\eta), v=-\frac{\partial\psi}{\partial x}=-\sqrt{av_f}f(\eta) \tag{19}$$

to reduce the governing equations (8)-(18) into boundary value problem to minimize the complexity of the problem. The reduced boundary value problem is given as,

$$\begin{aligned}&\frac{m_1}{m_2}f'''+f''f+\beta\left[2ff'f''-f^2f'''\right]+\frac{m_3}{m_2}M\sin^2(\gamma)[\beta ff''-f']-f'^2\\&+\delta(1+\beta_t\theta)\theta\cos(\alpha)=0\end{aligned} \tag{20}$$

$$\frac{m_5}{m_4}\frac{1}{Pr}(1+R_d)\theta''+f\theta'-f'\theta-f'\epsilon=0. \tag{21}$$

The modified boundary conditions are as follows:

$$f(0)=0, f'(0)=1, f'(\infty)=0, \theta'(0)=-\frac{Bi}{\frac{k_{nf}}{k_f}}(1-\epsilon-\theta(0)), \theta(\infty)=0. \tag{22}$$

From the equations (13)-(15), β indicates Deborah number , M denotes the magnetic number, δ depicts mixed convection parameter, β_t characterizes nonlinear convection number, Gr_x means Grashof number, Re_x symbolizes Reynolds parameter, Pr expresses the Prandtl number, ϵ identifies thermal stratification parameter, R_d signifies radiation parameter, Bi denotes Biot parameter, m_1, m_2, m_3, m_4, m_5 are dimensional constants. The aforementioned constraints are

$$\beta=\lambda_1 a, M=\frac{\sigma_f B_0^2}{\rho_f}, \delta=\frac{Gr_x}{Re_x^2}, \beta_t=\frac{\beta_2(T_f-T_0)}{\beta_1}, Gr_x=\frac{g\beta_1(T_f-T_0)x^3}{v_f^2}$$

$$Re_x=\frac{xu_w}{v_f}, Pr=\frac{(\mu c_p)_f}{k_f}, \mu_f=(\rho\nu)_f, \epsilon=\frac{a_1}{a_2}, R_a=\frac{16\sigma^* T_\infty^3}{3K^*(\rho Cp)_f},$$

$$Bi=\frac{h_f}{k_{nf}\sqrt{\frac{a}{v_f}}}, m_1=\mu_f\frac{1}{(1-\varphi)^{2.5}}, m_2=\rho_f\left[(1-\varphi)+\varphi\left(\frac{\rho_s}{\rho_f}\right)\right],$$

$$m_3=\sigma_f\left[\left(1+\frac{3\left(\frac{\sigma_s}{\sigma_f}-1\right)\varphi}{\left(\frac{\sigma_s}{\sigma_f}+2\right)-\left(\frac{\sigma_s}{\sigma_f}-1\right)\varphi}\right)\right], m_4$$

$$=(\rho Cp)_f\left[(1-\varphi)+\varphi\frac{(\rho Cp)_s}{(\rho Cp)_f}\right],$$

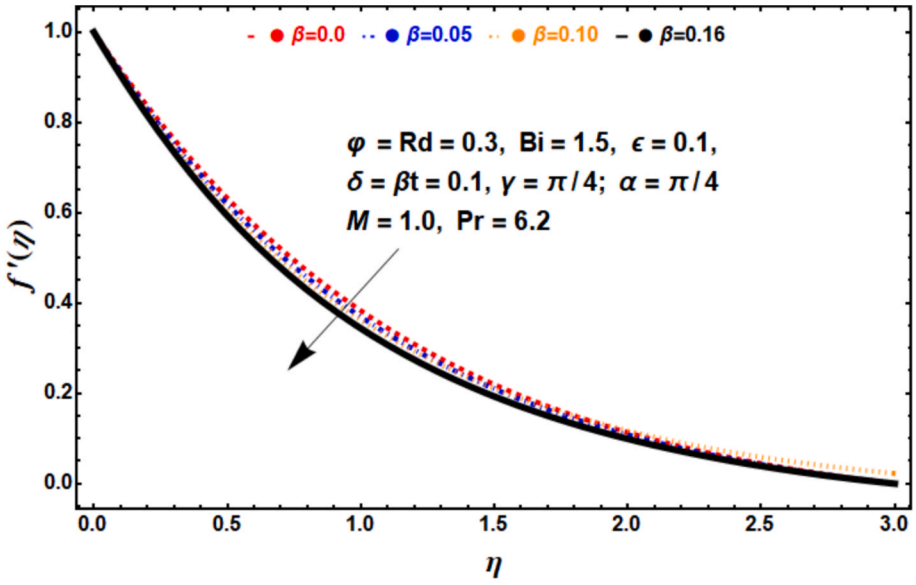

Fig. 2. Effect of β on the Velocity profile.

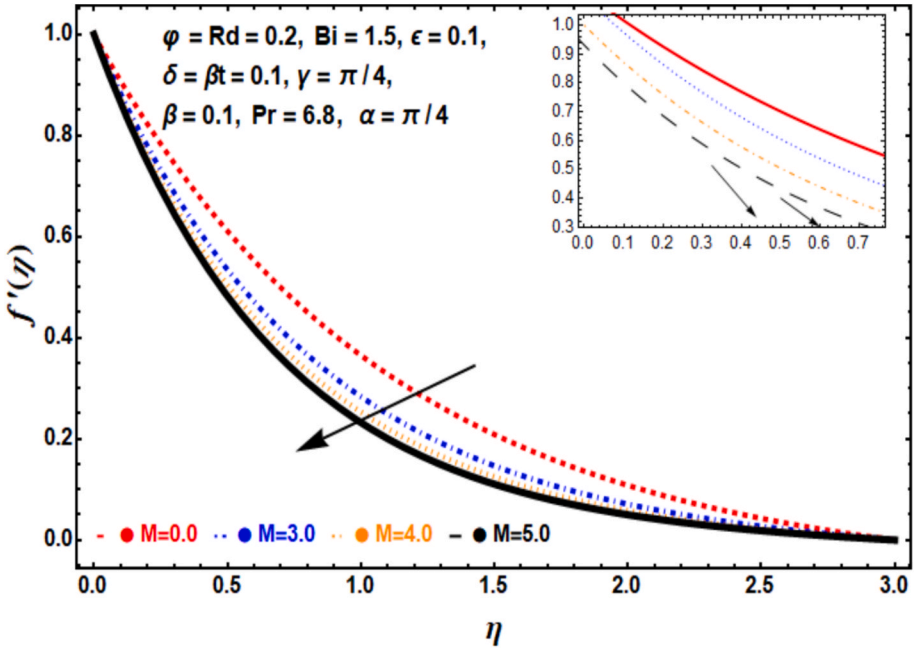

Fig. 3. Effect of M on the Velocity profile.

$$m_4 = k_f\left(\frac{k_s + 2k_f - 2\varphi(k_f - k_s)}{k_s + 2k_f + 2\varphi(k_f - k_s)}\right).$$

The quantities of physical interest are identified as skin friction and Nusselt number. The local skin-friction coefficient is defined by

$$Cf = \frac{\mu_{nf}\left(\frac{\partial u}{\partial y}\right)_{y=0}}{\rho_f u_w^2(x)/2}, \quad \frac{1}{2}(\mathrm{Re}_x)^{\frac{1}{2}}Cf_x = (1-\varphi)^{-2.5}f''(0) \tag{23}$$

The local Nusselt number is expressed as

$$Nu = \frac{-xk_{nf}\left(\frac{\partial T}{\partial y}\right)_{y=0}}{k_f(T_w - T_\infty)}, \; q_w = -k_{nf}\left(\frac{\partial T}{\partial y} + q_r\right)_{y=0}, \; (Re)^{\frac{-1}{2}}Nu = -\frac{k_{nf}}{k_f}(1+R)\left[\frac{1}{1-\epsilon}\right]\theta'(0), \tag{24}$$

where $\mathrm{Re} = xU_w/\nu_f$ demonstrating the Reynolds number.

3. Overview of the numerical approach

Due to the inherent coupling and nonlinearity of the governing equations, an analytical solution is intractable. Consequently, the ND-Solve tool in Mathematica is employed to solve the boundary value problem numerically. This robust numerical method, based on the

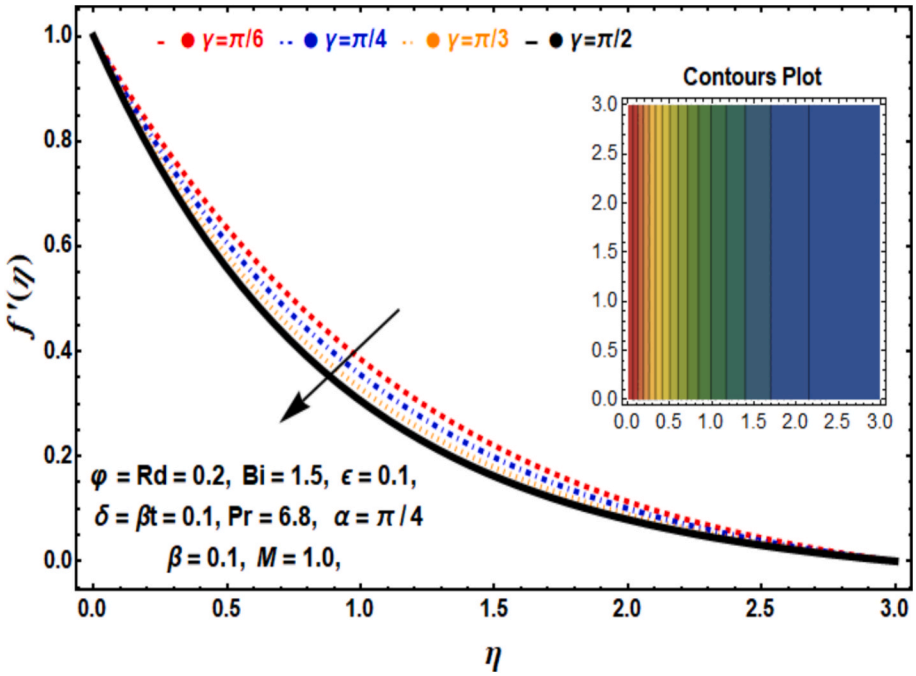

Fig. 4. Effect of γ on the Velocity profile.

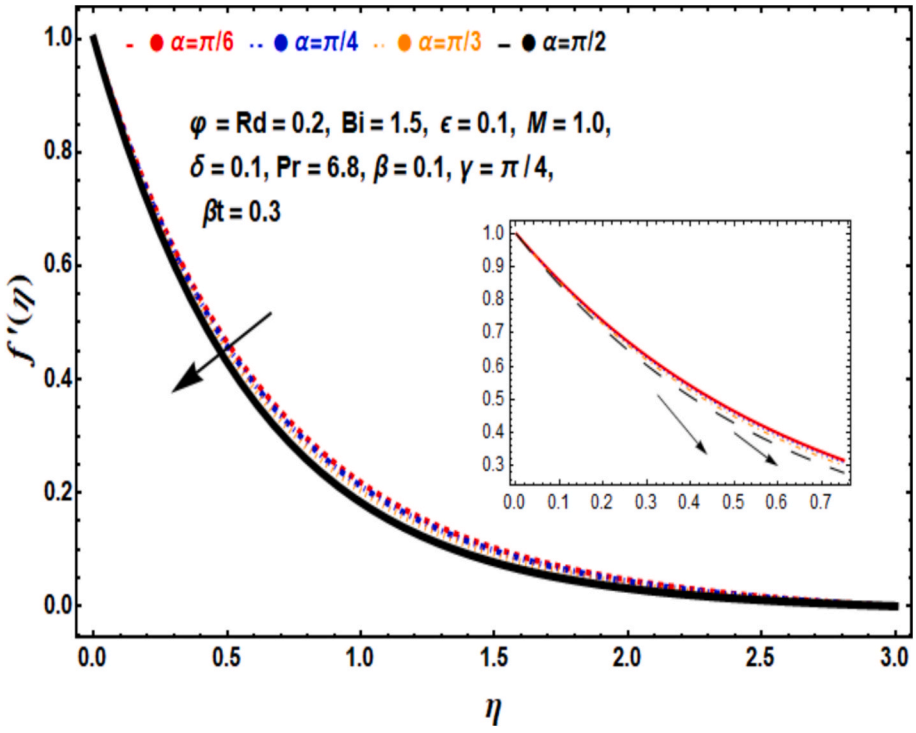

Fig. 5. Effect of α on the Velocity profile.

fourth-order Runge-Kutta technique, is widely used in scientific research.

Discretely assessing the data, the ND Solve function Mathematica's built-in package is used to numerically solve the system of equations (15)–(18). Figs. 2–20 present the findings. The system of ordinary differential equations (ODEs) is made up of a number of equations like $(M_1, M_2, M_3 \cdots M_n)$, where the dependent variables is η and the independent variables Ψ are $(L_1, L_2, L_3 \cdots L_n)$. The consequent computations are achieved using the ND-Solve function in Mathematica:

NDSolve $[\{M_1, M_2, M_3 \cdots M_n, bcs\}, \{L_1, L_2, L_3 \cdots L_\psi\}, \{\eta, \eta_{min}, \eta_{max}\}]$.

3.1. Validation of the numerical outcomes

Table. 2. Presents a comparison between the measured surface drag force and the benchmark data from [54]. The excellent agreement between the two validates the proposed model, providing a strong foundation for future research in this field.

The vital benefits of the technique applied here are:

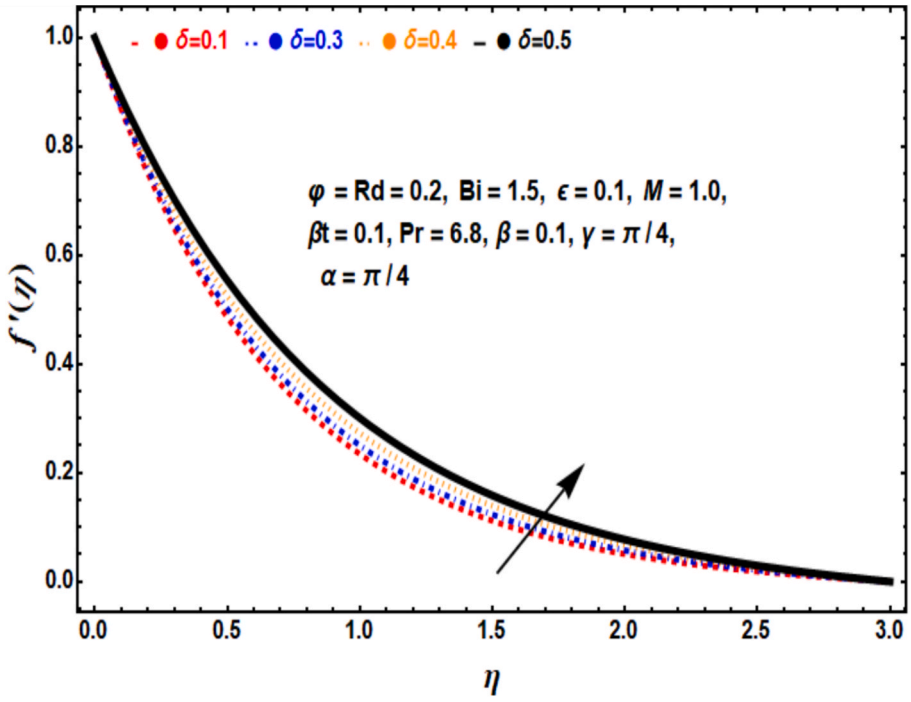

Fig. 6. Effect of δ on the Velocity profile.

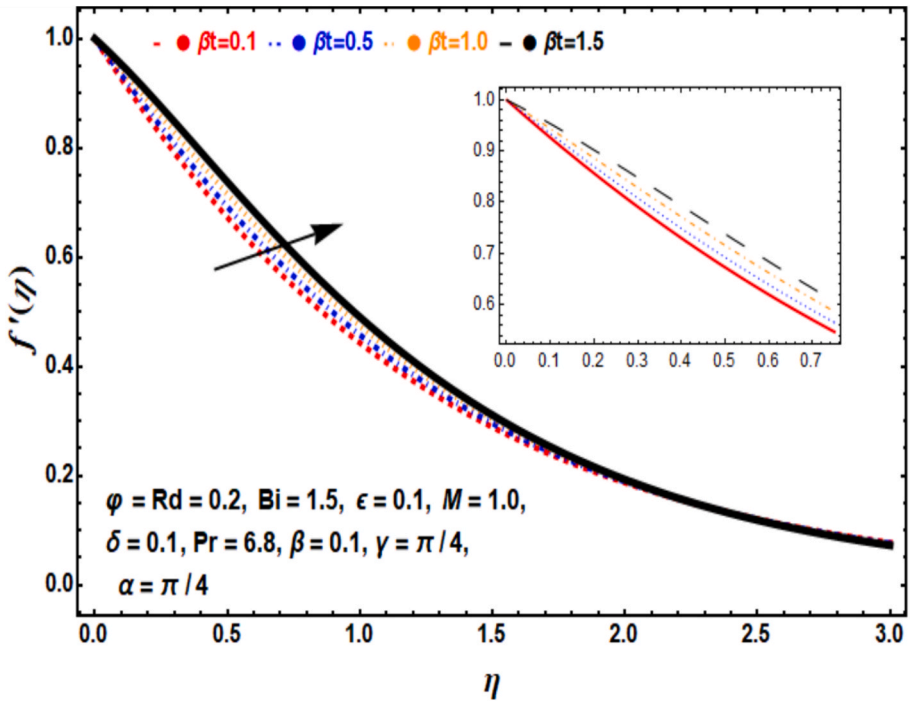

Fig. 7. Effect of β_t on the Velocity profile.

- It delivers highly accurate results.
- It requires less CPU time, improving efficiency.
- It is more robust and reliable for well-posed, real-world problems.

4. Results and discussion

This section illustrates various control factors that affect fluid flow and thermal profile through graphical representations. The affecting parameters are as follows: Deborah number (β=0.0, 0.05, 0.10, 0.15), magnetic field parameter (M = 1.0, 2.0, 3.0, 4.0), thermal Grashof number (δ = 0.3, 0.6, 1.0, 1.5), thermal convection parameter (β_t = 0.1, 0.3, 0.4, 0.5), thermal radiation parameter (R_d = 1, 3, 4, 5), thermal stratification parameter (ϵ = 0.1, 0.2, 0.3, 0.4), thermal Biot number (Bi = 0.2, 0.4, 0.6, 0.8) and Prandtl numbers (Pr = 0.72, 6.0, 6.8). This section aims to look at the graphical and physical properties of a few pertinent factors, like the temperature and velocity fields. Moreover, the behaviour of important variables of interest, namely the drag force coefficient and Nusselt number, is illustrated through table presentations.

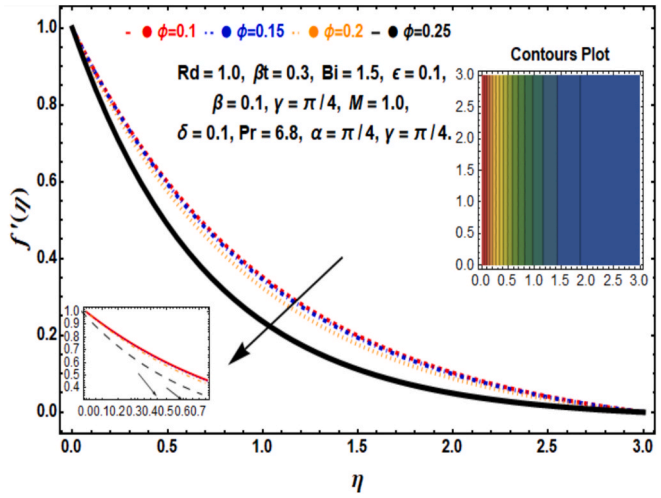

Fig. 8. Effect of nanoparticle volume fraction ϕ $(Fe_3O_4 + Siliconeoil)$ on Velocity profile.

The fluid velocity variation concerning variations in the Deborah number is adorned in Fig. 2. Based on the figure, the fluid's velocity decreases as the Deborah number improves. Physically, a higher degree of Deborah number indicates stronger viscoelastic effects, meaning the fluid holds more of its elastic memory. This increased elasticity enhances internal resistance, thickening the boundary layer and restricting the fluid's motion. As a result, the fluid experiences greater opposition to deformation, effectively increasing the apparent viscosity and reducing the overall velocity. The delayed flow response observed with increasing β highlights the fundamental role of viscoelasticity in modifying the transport characteristics of the nanofluid.

Fig. 3 illustrates the magnetic field's effect on the system's velocity profile. A magnetic field reduces the flow of fluid. This behaviour can be explained by the fact that a higher magnetic field directs to a decline in fluid momentum and a stronger Lorentz force, which, in turn, resists fluid movement. This finding finds practical applications in several technologies, such as MHD pumps and electromagnetic flow meters. A magnetic field is adapted to manipulate the flow of conductive fluids in the design of MHD pumps.

The consequence of the inclined angle γ on the velocity profile is portrayed in Fig. 4. The velocity profile exhibits a notable reduction with an increase in the inclination of the angle γ. Physically, a rise in the inclined angle γ causes the fluid to encounter more resistance during motion, which throws off the alignment of the flow and lowers the fluid's velocity. Fig. 5 shows that the velocity profile dramatically reduces as the angle of inclination α increases. Physically, the gravitational force opposing the fluid flow gets stronger as the angle of inclination α increases. The fluid's movement is slowed down by this additional resistance, which lowers the fluid's overall velocity.

Fig. 6 shows that the velocity profile falls with increasing mixed convection parameters. Physically, a greater mixed convection parameter improves buoyancy effects, which influence the force balance within the boundary layer. By adding more resistance to the fluid motion, buoyancy forces change the velocity gradient close to the surface. This higher resistance thickens the boundary layer, inhibits momentum transmission, and eventually lowers fluid velocity. This knowledge helps optimize fluid dynamics in heating, ventilation, and air conditioning (HVAC) units, where adequate ventilation and temperature management depend on velocity control. The impact of the thermal buoyancy parameter on the velocity profile is also seen in Fig. 7. Because of the stronger buoyant forces, the velocity increases as the thermal buoyancy parameter increases. By overcoming fluid resistance, these forces contribute significantly to increased fluid velocity and a wider momentum boundary layer. This realization emphasizes how crucial buoyancy-driven flow is for applications involving convective heat transfer.

Fluid velocity decreases as nanoparticle concentration rises, as seen in Figs. 8 and 9. This phenomenon is because of the increased viscosity in the nanofluid $(blood + Fe_3O_4)$ and nanofluid $(water + Fe_3O_4)$ enhances the barrier to flow. While adding nanoparticles improves thermal conductivity, the higher viscosity predominates and causes the fluid to move more slowly. Compared to $(water + Fe_3O_4)$, the $(blood + Fe_3O_4)$ shows a more significant reduction of velocity because of blood's higher viscosity, increasing flow resistance as nanoparticle concentration rises.

Fig. 10 shows that increasing the Deborah number leads to higher temperatures and a thicker thermal boundary layer. This is due to enhanced fluid elasticity at higher Deborah numbers, which impedes heat dissipation and leads to thermal energy buildup. Fig. 11 illustrates

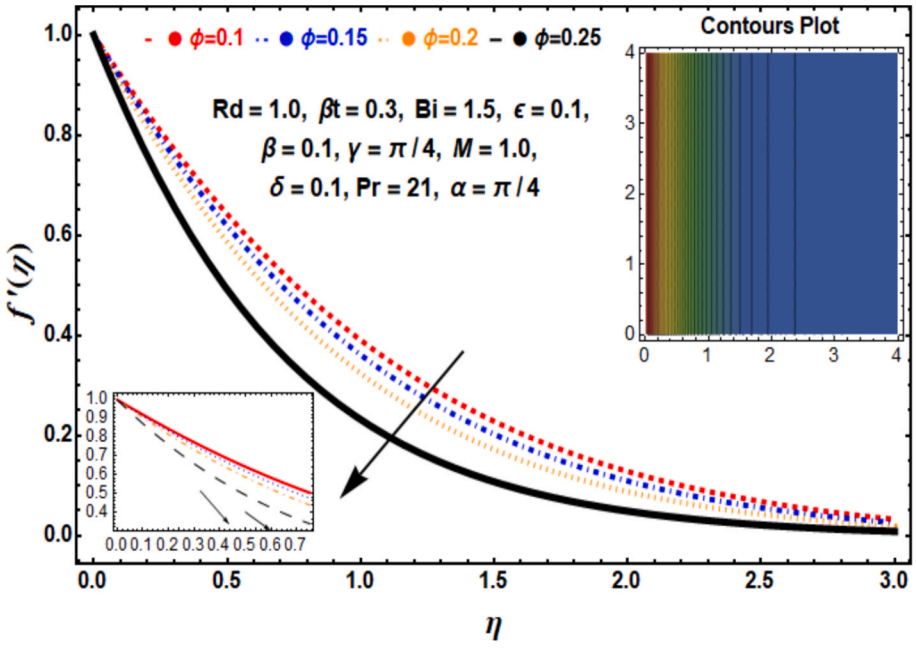

Fig. 9. Effect of nanoparticle volume fraction ϕ $(Fe_3O_4 + Blood)$ on Velocity profile.

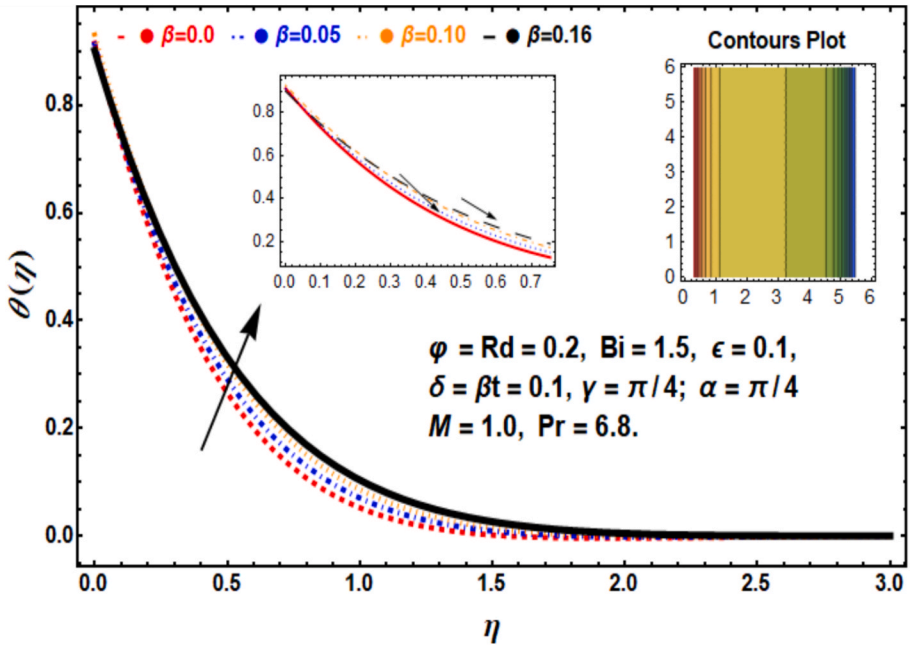

Fig. 10. Effect of β on the Temperature profile.

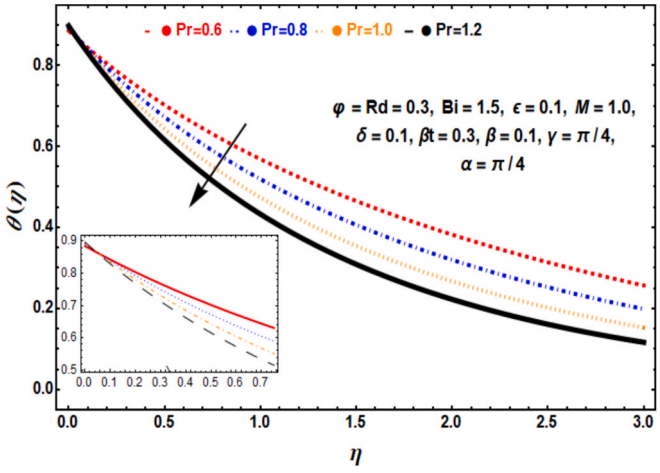

Fig. 11. Effect of *Pr* on the Temperature profile.

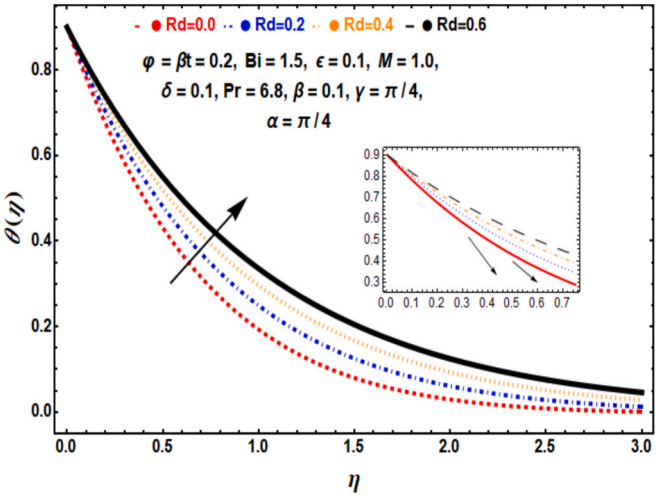

Fig. 13. Effect of R_d on the Temperature profile.

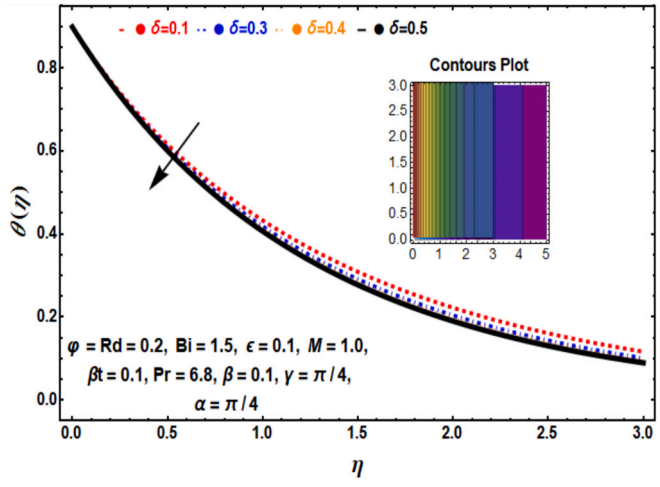

Fig. 12. Effect of δ on the Temperature profile.

the effect of the Prandtl number on the temperature profile. As the Prandtl number increases, the temperature decreases, and the thermal boundary layer becomes steeper. This is because higher Prandtl numbers correspond to lower thermal diffusivity, which reduces heat transfer. The Grashof number characterizes the relative strength of buoyancy and viscous forces, thereby governing convective heat transfer. As the fluid density decreases due to heating, buoyancy forces are enhanced, leading to increased particle kinetic energy.

As illustrated in Fig. 12, the temperature profile drops as the mixed convection parameter increase because of stronger natural convection effects. Buoyant forces become stronger as the mixed convection parameter rises, encouraging more heat loss and lowering the fluid's temperature. This leads to a thinner thermal boundary layer and improved heat transfer efficiency. The trend is further supported by the Nusselt number, which increases with higher δ, indicating enhanced convective heat transfer. Such behavior is essential in HVAC applications, where temperature regulation and ventilation efficiency are enhanced by utilizing natural convection.

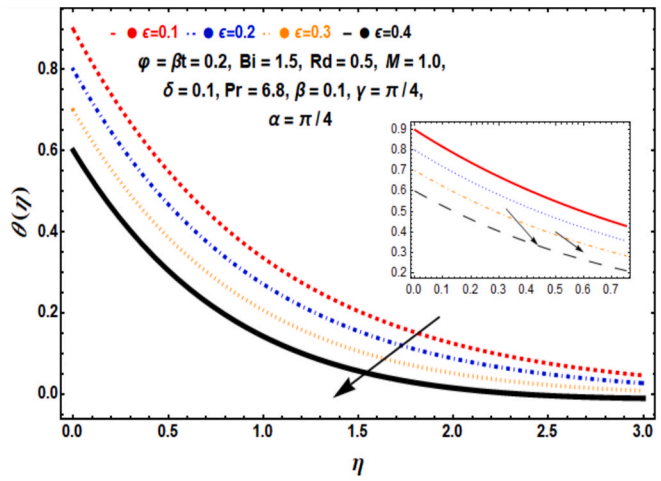

Fig. 14. Effect of ϵ on the Temperature profile.

Fig. 13 shows that increasing the radiation parameter leads to an increase in both temperature and thermal boundary layer thickness. This occurrence is because the heated plate emits heat, which makes the thermal field stronger. When a higher temperature is needed, the radiation effect comes in handy. On the other hand, the radiation parameter becomes less significant when further from the boundary.

Fig. 14 shows that increasing the stratification parameter leads to a decrease in both temperature and thermal boundary layer thickness. Physically, higher thermal stratification results in increased fluid density near the lower surface. This increased resistance to heat transfer from the heated wall leads to lower temperatures in the surrounding area. Fig. 15 illustrates the effect of the Biot number on the temperature field. As the Biot number increases, both temperature and thermal boundary layer thickness increase. A higher Biot number signifies enhanced heat transfer between the fluid and the heated surface, leading to increased heat absorption by the fluid and a more pronounced temperature profile. This phenomenon is especially advantageous when a greater surface temperature is necessary. Nevertheless, the Biot parameter's effect becomes less noticeable when one gets farther from the boundary.

The temperature profile decreases as the nanoparticle volume fraction rises, as shown in Figs. 16 and 17. This behaviour results from the interaction between the concentration of Fe_3O_4 nanoparticles in the nanofluid $(Blood + Fe_3O_4)$ and nanofluid $(Water + Fe_3O_4)$ and their thermal conductivity. Higher concentrations of Fe_3O_4 nanoparticles cause particle interactions that hinder thermal dispersion, even if they initially improve heat transfer by increasing thermal conductivity and aiding heat distribution. As a result, the overall heat transfer rate is significantly decreased, which lowers the temperature profile. The diminution is more noticeable in nanofluid $(Blood + Fe_3O_4)$ than nanofluid $(Water + Fe_3O_4)$ due to blood's greater viscosity. Blood's natural viscosity slows fluid mobility, usually permitting more heat retention. Effective heat transfer is further limited to higher nanoparticle concentrations due to the increasing flow resistance. The temperature profile significantly decreases as a result of this dual impact, which emphasizes the delicate balance between nanoparticle concentration and thermal performance in nanofluid systems. This occurrence is caused by slower fluid dynamics and reduced thermal dispersion by nanoparticle interactions.

Fig. 18a and 18b illustrate the impact of nanoparticle volume fraction and magnetic parameter on the skin friction coefficient. The results reveal a significant decrease in skin friction with increasing values of these parameters. This behavior can be attributed to the enhanced resistive effects of the Lorentz force and increased viscosity caused by higher nanoparticle concentrations, leading to reduced fluid velocity near the surface.

Fig. 19a and 19b, along with their 3D representations, illustrate the thermal Biot number and the thermal stratification parameter effect towards the Nusselt number. The findings show that both parameters raise the Nusselt number, though in different ways. While an increase in thermal stratification parameter increases the fluid's thermal gradient and promotes more effective heat dissipation, a rise in thermal Biot number strengthens convective boundary effects and improves heat transfer near the surface. These findings demonstrate how important boundary and stratification affect maximizing thermal performance.

Table. 3 presents the influence of the Deborah number, mixed convection parameter, and nanoparticle volume fraction on skin friction. The results indicate that skin friction increases with increasing values of these parameters. Physically, higher Deborah numbers, mixed

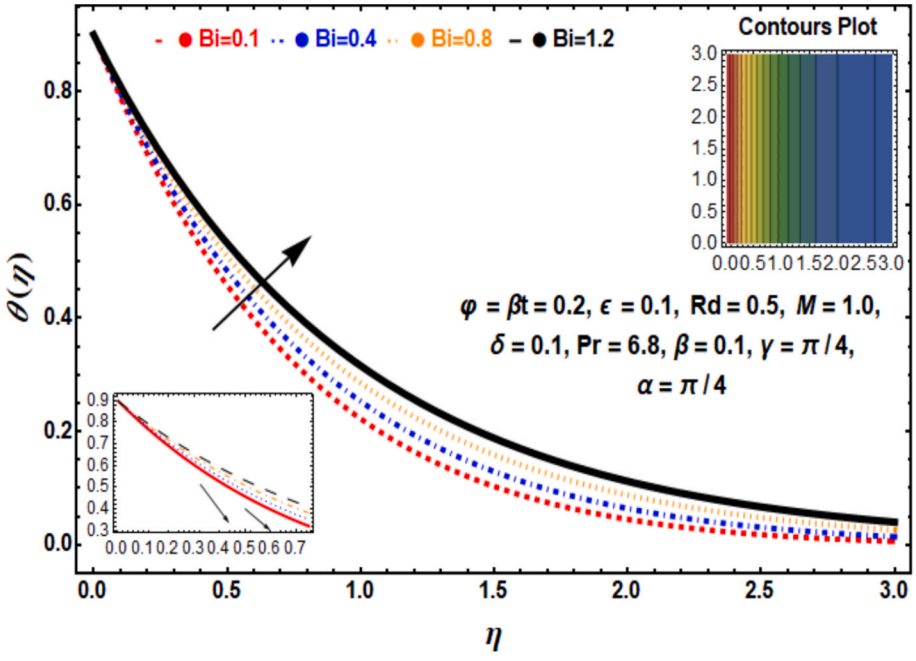

Fig. 15. Effect of *Bi* on the Temperature profile.

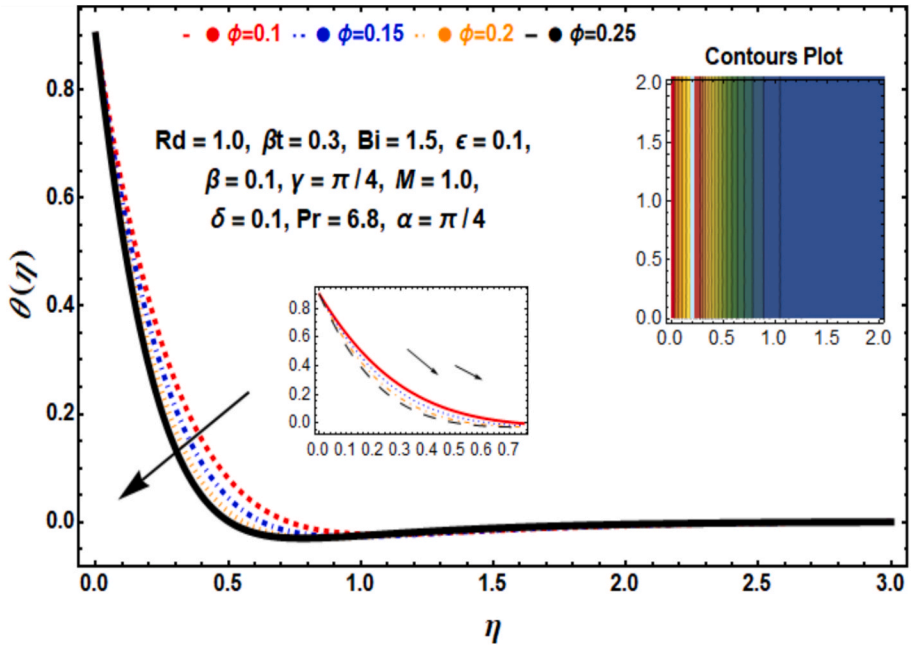

Fig. 16. Effect of nanoparticle volume fraction ϕ $(Fe_3O_4 + Siliconeoil)$ on Temperature profile.

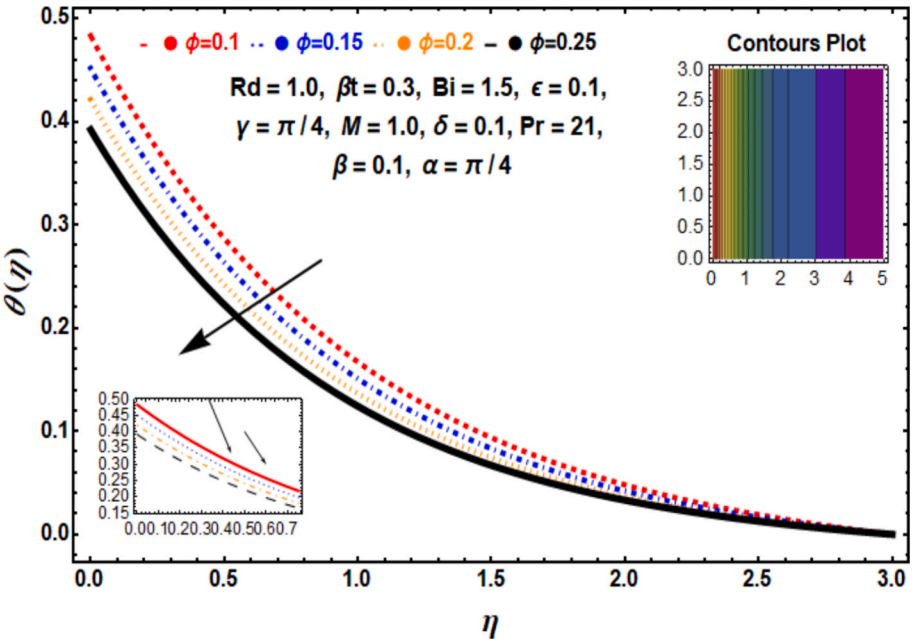

Fig. 17. Effect of nanoparticle volume fraction ϕ $(Fe_3O_4 + Blood)$ on Temperature profile.

convection, and nanoparticle volume fractions enhance frictional forces, leading to increased surface resistance. Conversely, a stronger magnetic field generates a Lorentz force that opposes fluid flow, resulting in reduced skin friction. Table. 4 demonstrates the impact of radiation, thermal stratification, thermal Biot number, nanoparticle volume fraction, magnetic parameter, and Deborah number on the Nusselt number. The findings indicate that the Nusselt number falls as nanoparticle volume fraction, magnetic, and Deborah numbers grow. However, it increases with larger radiation values, thermal stratification and thermal Biot number. Physically, by enhancing radiation, thermal stratification, and surface heat exchange, raising radiation parameters, thermal stratification parameters, and thermal Biot number improves heat transfer. On the other hand, greater values of the variables nanoparticle volume fraction, magnetic parameter and Deborah number (fluid elasticity) result in increased flow resistance, which in turn lowers the Nusselt number by decreasing the efficiency of convective heat transfer.

5. Conclusion

A novel study has been carried out to examine the effects of radiation, quadratic mixed convection, and thermal stratification on a non-Newtonian fluid over an inclined stretched surface is carried out, and a detailed examination of the interacting effects yields the following conclusions:

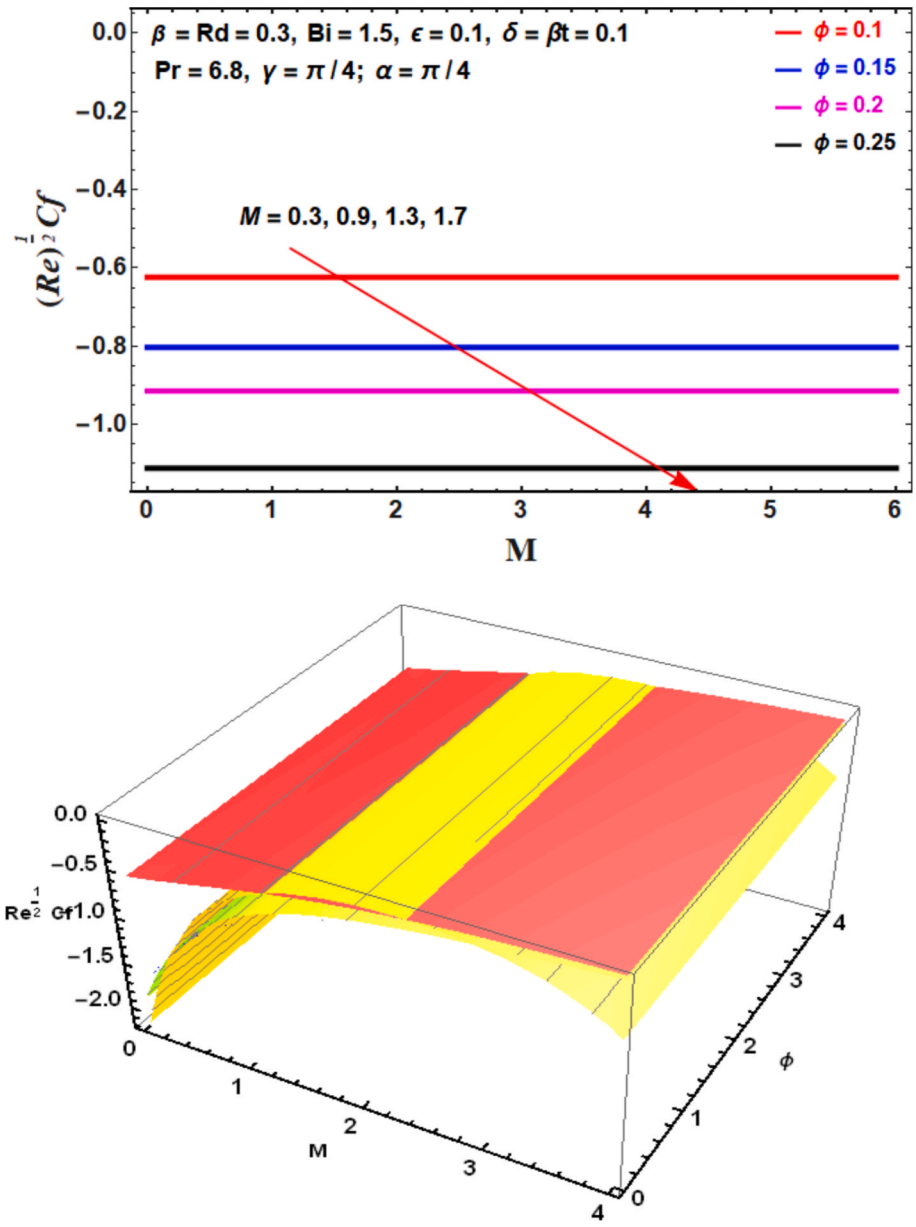

Fig. 18. A. effect of ϕ and M on $(Re)^{1/2}Cf$. b. 3D impact of ϕ and M on $(Re)^{1/2}Cf$.

- A higher Deborah number raises temperature profiles while decreasing velocity profiles.
- The temperature profile is lowered by a more significant Prandtl number and thermal stratification but raised by radiation.
- Higher concentrations of Fe_3O_4 nanoparticles boost the temperature profile but decrease the velocity profile, especially in nanofluid (blood-Fe_3O_4).
- Higher Grashof numbers enhance convective heat transfer, which lowers the temperature profiles while increasing fluid velocity due to increased buoyant forces.
- More significant nanoparticle volume fraction, Deborah number, and mixed convection parameters increase skin friction, but greater magnetic parameter values cause skin friction to decrease.
- Higher radiation values, thermal stratification, and thermal Biot number cause the Nusselt number to increase, while rising nanoparticle volume fraction, Deborah number, and mixed convection parameters cause it to drop.

5.1. Practical applications of proposed model

Energy-saving transportation is made possible by thermal stratification using nanofluids, hybrid, and trihybrid nanofluids under strong magnetic fields. This strategy has important ramifications for several applications, including industrial operations like heat exchangers and cooling systems, medical devices like drug delivery systems and thermal therapies, and renewable energy technologies like solar heating and HVAC systems. The advantages of stratification in these circumstances can boost performance and efficiency in thermal management.

5.2. Future work

Future investigation can focus on experimental validation to fortify the accuracy and practical applicability of the findings. Furthermore, investigating different nanoparticles with diverse thermo-physical properties could enhance the efficacy and flexibility of nanofluids in innumerable industrial applications. This would offer deeper understanding into maximizing heat transfer performance for wider

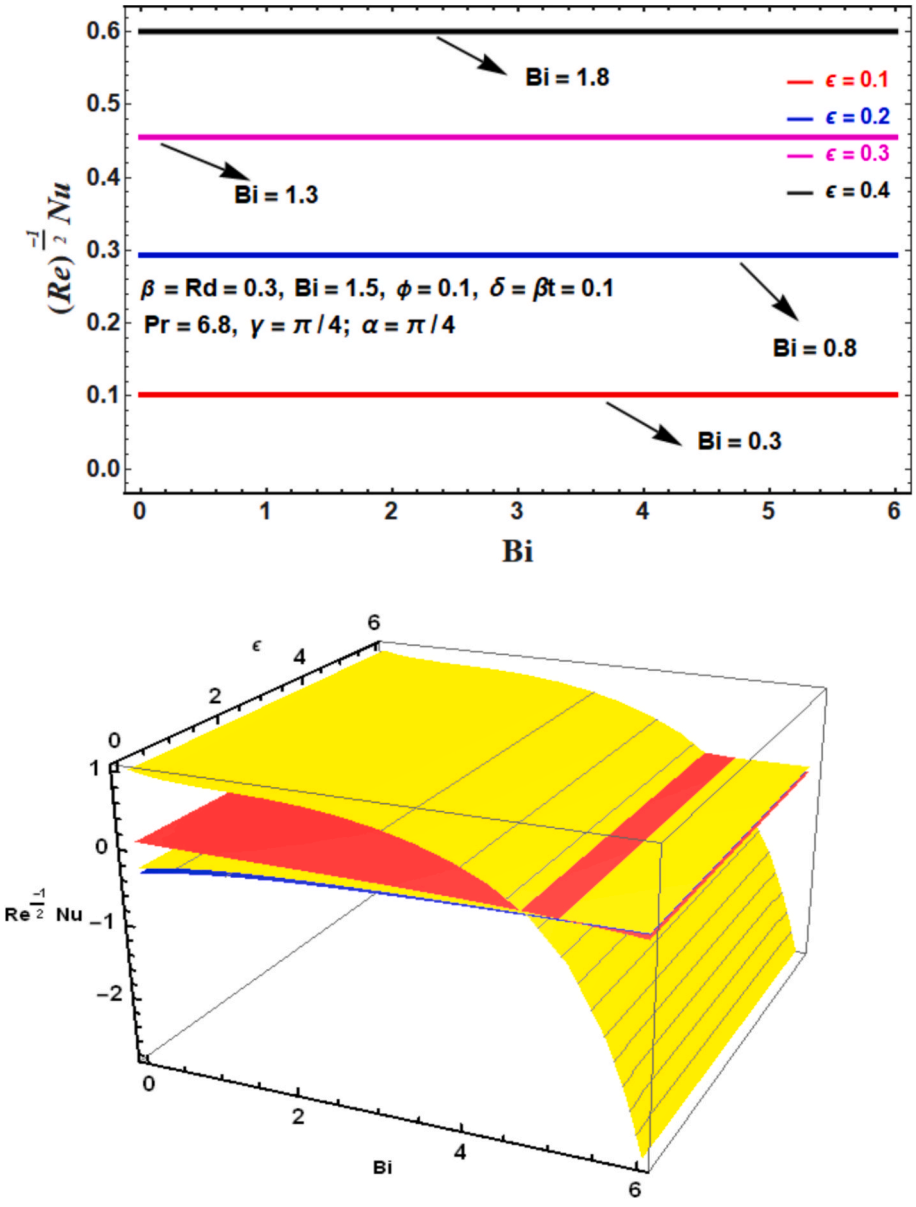

Fig. 19. B. effect of *Bi* and ϵ on $(Re)^{\frac{-1}{2}}Nu$. b. 3D impact of *Bi* and ϵ on $(Re)^{\frac{-1}{2}}Nu$.

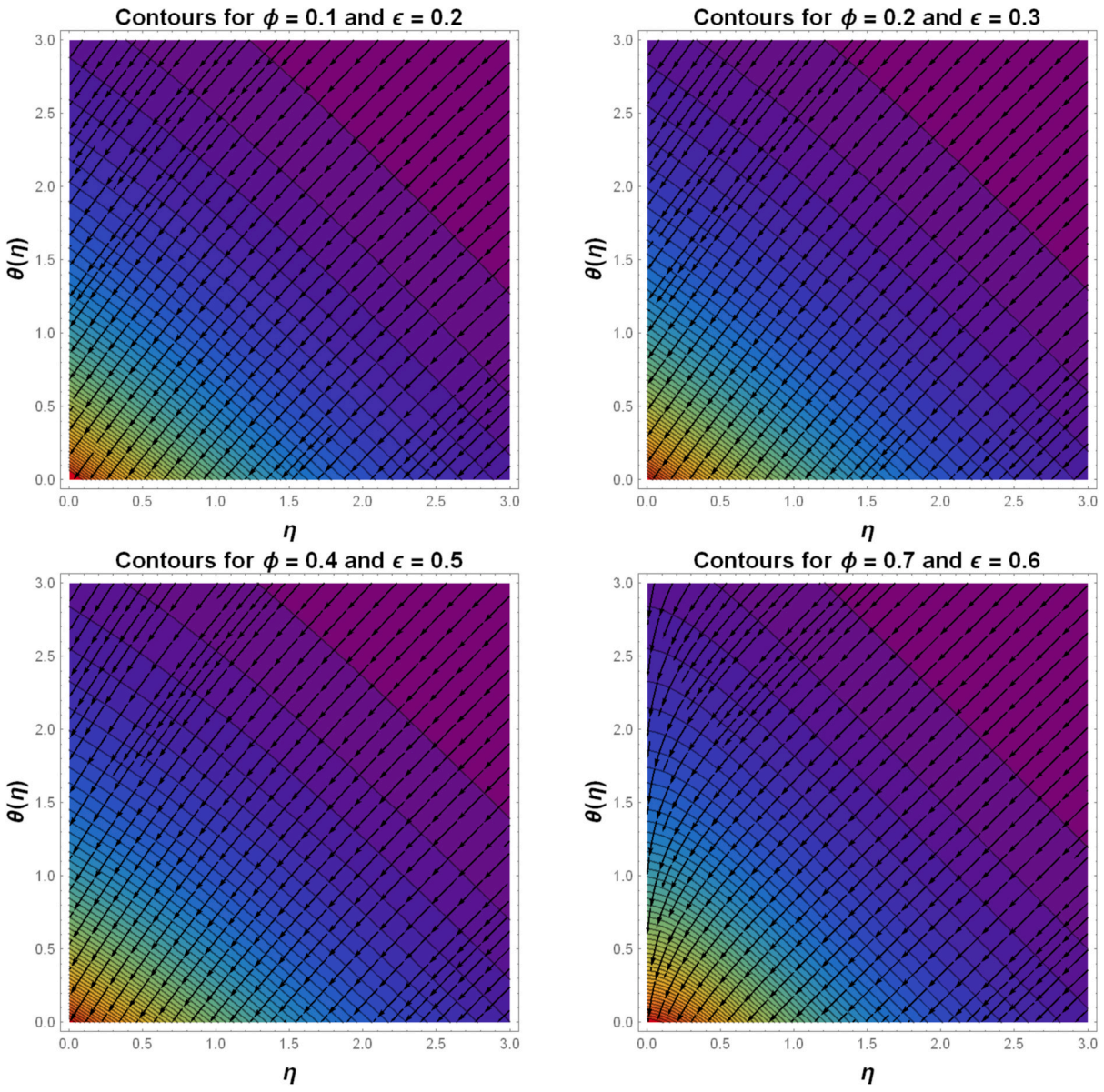

Fig. 20. Contours plot for ϕ and $\in$.

Table 2

Evaluation of the existing outcomes of $(Re)^{\frac{1}{2}}Cf$ with the Previous literature Ahmad et al. [54] for various values of M.

M	$(Re)^{\frac{1}{2}}Cf$ Ahmad et al. [54]	Present study
1	0.822969	−1.0265
2	0.511285	−1.0513
3	0.19812	−1.0757
4	−0.116521	−1.0996

Table 3

Numerical values for skin friction coefficients for different values.

β	M	δ	φ	$f''(0)$
0.1				−1.9994
0.2				−1.5678
0.3				−1.5811
0.4				−1.5944
	1			−1.0265
	2			−1.0513
	3			−1.0757
	4			−1.0996
		0		−1.637
		0.5		−2.0709
		1		−1.5783
		1.2		−1.5493
			0.0	−2.4099
			0.1	−2.3443
			0.2	−2.28059
			0.3	−2.21886

engineering and scientific advancements.

Limitations of the study

While this research offers remarkable insights into the effects of nonlinear mixed convection and quadratic stratification in non-Newtonian nanofluid flow, certain limitations should be acknowledged to refine its scope and applicability:

i Idealized boundary conditions

A two-dimensional, steady-state flow model with particular

Table 4
Numerical values for Nusselt number coefficients for different values.

M	β	R_d	ϵ	Bi	φ	$\theta'(0)$
0.1						1.8488
0.2						1.8327
0.3						1.8171
0.4						1.8019
	1					1.5567
	2					1.5469
	3					1.5374
	4					1.5281
		0.0				1.3712
		0.1				1.4957
		0.2				1.6203
		0.3				1.745
			0.0			2.0966
			0.1			2.3587
			0.2			2.6957
			0.3			3.145
				0.0		1.3746
				0.1		1.7691
				0.2		1.9656
				0.3		2.0721
					0.0	−2.2781
					0.1	−2.3349
					0.2	2.3928
					0.3	−2.4516

boundary conditions serves as the basis for the study, which might not adequately represent transient or three-dimensional phenomena that arise in practical applications.

ii Lack of experimental validation

Although our numerical findings align with established benchmarks, experimental validation is not included in this study. Future comparisons with experimental data would further reinforce the reliability of our results.

iii Simplified nanofluid properties

The thermophysical properties of the nanofluid are assumed constant, whereas, in real-world applications, temperature-dependent variations, nanoparticle aggregation, and interfacial interactions could impact heat transmission performance.

iv Ignoring the impact of turbulence

The study concentrates on a laminar flow regime, however turbulence is a prominent factor in many industrial and environmental applications, and it has a considerable impact on the dynamics of heat and mass transfer.

v Single-Phase nanofluid model

It uses a single-phase nanofluid method, which ignores factors like thermophoretic effects, Brownian motion, and nanoparticle migration that could change transport phenomena in a more thorough two-phase model.

CRediT authorship contribution statement

Abbas Khan: Writing – review & editing. **Hashim:** Writing – review & editing. **Muhammad Farooq:** Writing – review & editing. **Wasim Jamshed:** Writing – original draft, Methodology. **Basim M. Makhdoum:** Writing – review & editing. **Nor Ain Azeany Mohd Nasir:** Methodology.

Funding

This research work was funded by Umm Al-Qura University, Saudi Arabia under grant number: 25UQU4331007GSSR01.

Declaration of competing interest

The authors declare that they have no known competing financial interests or personal relationships that could have appeared to influence the work reported in this paper.

Acknowledgment

The authors extend their appreciation to Umm Al-Qura University, Saudi Arabia for funding this research work through grant number: 25UQU4331007GSSR01.

References

[1] Mohammadpour J, Salehi F, Lee A, Brandt L. Nanofluid heat transfer in a microchannel heat sink with multiple synthetic jets and protrusions. *Int J Therm Sci*, 2022;179:107642.
[2] Khan AA, Ahmed A, Askar S, Ashraf M, Ahmad H, Khan MN. Influence of the induced magnetic field on second-grade nanofluid flow with multiple slip boundary conditions. *Waves Random Complex Media* 2021:1–16.
[3] Jamil B, Anwar MS, Rasheed A, Irfan M. MHD Maxwell flow modeled by fractional derivatives with chemical reaction and thermal radiation. *Chin J Phys*, 2020;67:512–33.
[4] Hayat T, Khan SA, Khan MI, Alsaedi A. Optimizing the theoretical analysis of entropy generation in the flow of second grade nanofluid. *Phys Scr*, 2019;94(8):085001.
[5] Anwar MS, Rasheed A. Simulations of a fractional rate type nanofluid flow with non-integer Caputo time derivatives. *Comput Math Appl*, 2017;74(10):2485–502.
[6] Shoaib Anwar M, Rasheed A. Heat transfer at microscopic level in a MHD fractional inertial flow confined between non-isothermal boundaries. *Eur Phys J plus* 2017;132:1–17.
[7] Rasheed A, Anwar MS. Numerical computations of fractional nonlinear Hartmann flow with revised heat flux model. *Comput Math Appl*, 2018;76(10):2421–33.
[8] Qureshi HZ, Ahmad I. Neural network knacks to investigate thermal variability in nanofluidic fin through temperature-dependent analysis and heat generation studies. *Eur Phys J plus* 2024;139(8):720.
[9] Pavan Kumar P, Gireesha B, Venkatesh P, Keerthi M. Transient thermal behavior and efficiency in fully wet porous longitudinal fin: The influence of shape-dependent hybrid nanofluid and internal heat generation. *Numer Heat Transf Part Appl*, 2024:1–21.
[10] Rokhforouz M, Sheikholeslami M. Numerical investigation of the process of melting and solidification within a parabolic trough solar collector using nanoparticles and fins. *J Clean Prod*, 2024;434:140269.
[11] Awais M, Hayat T, Ali A, Irum S. Velocity, thermal and concentration slip effects on a magneto-hydrodynamic nanofluid flow. *Alex Eng J*, 2016;55(3):2107–14.
[12] De Souze S, Job VM, Narayana M. Ferrohydrodynamic mixed convection in Fe $_3 O_4 -water/EG or Ni_3 $ Fe-water/EG ferrofluid in a porous square vented enclosure. *Eur Phys J plus* 2024;139(2):1–18.
[13] Khan SS, Mushtaq M, Jabeen K. Mixed convection and double diffusion impacts on Williamson–Sutterby nanofluid with activation energy, Cattaneo–Christov heat flux, and a magnetic dipole. *Arab J Sci Eng*, 2024;49(8):10523–45.
[14] Sivakumar N, Noeiaghdam S, Fernandez-Gamiz U. and others, "Multiple shape factor effects of nanofluids on marangoni mixed convection flow through porous medium,". *Results Eng*, 2024;23:102512.
[15] Awang N, Ab Raji NH, Rahim AA, Ilias MR, Shafie S, Ishak SS. Nanoparticle Shape Effects of Aligned Magnetohydrodynamics Mixed Convection Flow of Jeffrey Hybrid Nanofluid over a Stretching Vertical Plate. *J Adv Res Appl Mech*, 2024;112(1):88–101.
[16] Ahmad S, Akhter S, Shahid MI, Ali K, Akhtar M, Ashraf M. Novel thermal aspects of hybrid nanofluid flow comprising of manganese zinc ferrite MnZnFe2O4, nickel zinc ferrite NiZnFe2O4 and motile microorganisms. *Ain Shams Eng J*, 2022;13(5):101668.
[17] Bin Mizan MR, Ferdows M, Shamshuddin M, Bég OA, Salawu SO, Kadir A. Computation of ferromagnetic/nonmagnetic nanofluid flow over a stretching cylinder with induction and curvature effects. *Heat Transf*, 2021;50(6):5240–66.
[18] Rajarathinam M, et al. Combined buoyancy and Marangoni convective heat transport of CNT-water nanofluid in an open chamber with influence of magnetic field and isothermal solid block. *Partial Differ Equ Appl Math*, 2024;12:101005.
[19] Sarma AK, Sarma D. Unsteady magnetohydrodynamic bioconvection Casson fluid flow in presence of gyrotactic microorganisms over a vertically stretched sheet. *Numer Heat Transf Part Appl*, 2024:1–24.
[20] I. K. Aljohani and A. S. Omer, "Artificial Neural Computing and Statistical Analysis of Heat and Mass Transport of Nanofluid Flow with Melting Heat and Thermal Stratification".
[21] Hussain Z, Hussain A, Anwar MS, Farooq M. Analysis of Cattaneo–Christov heat flux in Jeffery fluid flow with heat source over a stretching cylinder. *J Therm Anal Calorim*, 2022;147(4):3391–402.
[22] Irfan M, Khan M, Khan W. Behavior of stratifications and convective phenomena in mixed convection flow of 3D Carreau nanofluid with radiative heat flux. *J Braz Soc Mech Sci Eng*, 2018;40(11):521.
[23] Hussain Z, Hayat T, Alsaedi A, Anwar MS. Mixed convective flow of CNTs nanofluid subject to varying viscosity and reactions. *Sci Rep*, 2021;11(1):22838.
[24] Jha BK, Samaila G. Nonlinear Approximation for Natural Convection Flow Past A Vertical Moving Plate With Nonlinear Thermal Radiation Effect. *J Model Simul Mater*, 2024;6(1):1–10.
[25] Mahanthesh B, Joseph T, Thriveni K. Dynamics of non-Newtonian nanoliquid with quadratic thermal convection. *Math Fluid Mech*, 2021:223–48.

[26] Al-Kouz W, Mahanthesh B, Alqarni M, Thriveni K. A study of quadratic thermal radiation and quadratic convection on viscoelastic material flow with two different heat source modulations. *Int Commun Heat Mass Transf*, 2021;126:105364.
[27] Khedher NB, El-Zahar ER, Seddek LF, Ullah Z, Eldin SM. Amplitude and oscillating assessment of thermal and magnetic boundary layer flow across circular heated cylinder with heat source/sink. *Case Stud Therm Eng*, 2023;49:103216.
[28] Ullah Z, et al. Thermal radiation and soret/dufour effects on amplitude and oscillating frequency of darcian mixed convective heat and mass rate of nanofluid along porous plate. *Case Stud Therm Eng*, 2024;59:104562.
[29] Jha BK, Oni MO. Theory of fully developed mixed convection including flow reversal: a nonlinear Boussinesq approximation approach. *Heat Transfer—Asian Res*, 2019;48(8):3477–88.
[30] Shaheen A, Waqas H, Imran M, Raza M, Rashid S. The effects of thermal radiation and heat source/sink on the flow and heat transfer characteristics of a hybrid nanofluid over a vertical stretching cylinder: Regression analysis. *Int J Mod Phys B* 2024;38(29):2450397.
[31] Shaheen A, Hasan MJ, Imran M, Waqas H, Muhammad T. Hydrothermal properties with entropy generation effects on a hybrid nanofluid considering thermal radiation on a stretching/shrinking sheet. *Numer Heat Transf Part Appl*, 2024:1–22.
[32] S. Muhammad Raza Shah Naqvi *et al.*, "Numerical investigation of thermal radiation with entropy generation effects in hybrid nanofluid flow over a shrinking/stretching sheet," *Nanotechnol. Rev.*, vol. 13, no. 1, p. 20230171, 2024.
[33] Jamir T, Konwar H, Tzudir B. Soret and dufour effects on unsteady non-linear mixed convection flow past a stretching sheet influenced by non-linear thermal radiation. *Numer Heat Transf Part Appl*, 2024:1–19.
[34] Mandal G, Pal D. Mixed convective-quadratic radiative MoS 2–SiO 2/H 2 O hybrid nanofluid flow over an exponentially shrinking permeable Riga surface with slip velocity and convective boundary conditions: entropy and stability analysis. *Numer Heat Transf Part Appl*, 2024;85(14):2315–40.
[35] Yahaya RI, et al. Mixed convection hybrid nanofluid flow over a stationary permeable vertical cone with thermal radiation and convective boundary condition. *ZAMM-J Appl Math Mech Für Angew Math Mech*, 2024;104(4): e202300428.
[36] Skerget L. *Mixed Convection Cavity Flows*, vol. 19. WIT Press; 2024.
[37] Alzahrani SM, Alzahrani TA. Enhanced Efficiency of MHD-Driven Double-Diffusive Natural Convection in Ternary Hybrid Nanofluid-Filled Quadrantal Enclosure: A Numerical Study. *Mathematics* 2024;12(10):1423.
[38] Geetha R, Reddappa B, Tarakaramu N, Rushi Kumar B, Ijaz Khan M. Effect of Double Stratification on MHD Williamson Boundary Layer Flow and Heat Transfer across a Shrinking/Stretching Sheet Immersed in a Porous Medium. *Int J Chem Eng*, 2024;2024(1):9983489.
[39] Suganthi R, Pullepu B, Supriya P, Shanmugapriya M, Pop I. Variable thermal conductivity and mass diffusivity effects in a free convective flow of doubly stratified non-darcian porous medium over a vertical plate. *Int J Appl Mech Eng*, 2024;29(1):159–78.
[40] Mutuku WN, Makinde OD. Double stratification effects on heat and mass transfer in unsteady MHD nanofluid flow over a flat surface. *Asia Pac J Comput Eng*, 2017;4: 1–16.
[41] Chetteti RR, Srivastav A. Double stratification in the flow of a Newtonian fluid along an inclined permeable stretching surface. *Adv Model Anal A* 2021;58(1–4): 1–5.
[42] Mallawi F, Bhuvaneswari M, Sivasankaran S, Eswaramoorthi S. Impact of double-stratification on convective flow of a non-Newtonian liquid in a Riga plate with Cattaneo-Christov double-flux and thermal radiation. *Ain Shams Eng J*, 2021;12(1): 969–81.
[43] Bilal M, Ramzan M, Mehmood Y, Kbiri Alaoui M, Chinram R. An entropy optimization study of non-Darcian magnetohydrodynamic Williamson nanofluid with nonlinear thermal radiation over a stratified sheet. *Proc Inst Mech Eng Part E J Process Mech Eng*, 2021;235(6):1883–94.
[44] Bilal S, Riaz MB. and others, "Thermofluidic transport of Williamson flow in stratified medium with radiative energy and heat source aspects by machine learning paradigm,". *Int J Thermofluids* 2024;24:100818.
[45] Bilal S, Riaz MB. and others, "Evaluating energy transmission characteristics of Non-Newtonian fluid flow in stratified and non-stratified regimes: A comparative study,". *Results Eng*, 2024;22:102157.
[46] Naduvinamani N, Basha H, Shridhar M. Stratified numerical heat and mass transport mechanism in MHD Maxwell fluid flow with nonuniform heat source/ sink. *Mod Phys Lett* 2024;B:2450442.
[47] Kanchana M. Influence of Cattaneo-Christov Heat Flux Model Rotating Maxwell Nanofluid with MHD and Double Stratification Across a Bidirectional Stretching Surface. *Commun Appl Nonlinear Anal*, 2024;31(6s):355–66.
[48] Khan KA, et al. Exploring the numerical simulation of Maxwell nanofluid flow over a stretching sheet with the influence of chemical reactions and thermal radiation. *Results Phys*, 2024;60:107635.
[49] R. Lakshmi and M. Kanchana, "THREE-DIMENSIONAL ROTATING SURFACE WITH THERMOPHORESIS AND VARIABLE THERMAL CONDUCTIVITY IN MAXWELL NANOFLUID".
[50] Naik LS, Prakasha D, Praveena M, Krishnamurthy M, Ganesh Kumar K. Stratification flow and variable heat transfer over different non-Newtonian fluids under the consideration of magnetic dipole. *Int J Mod Phys B* 2024;38(05): 2450071.
[51] N. Kalita, H. Kumar, R. S. Nath, and R. K. Deka, "Unsteady flow past an impulsively started infinite vertical plate in presence of thermal stratification and chemical reaction," *Heat Transf.*.
[52] Nath RS, Deka RK. Thermal and mass stratification effects on MHD nanofluid past an exponentially accelerated vertical plate through a porous medium with thermal radiation and heat source. *Int J Mod Phys* 2024;B:2550045.
[53] Hussain M, Lin D, Waqas H, Jiang F, Muhammad T. Advanced thermal performance of blood-integrated tri-hybrid nanofluid: an artificial neural network-based modeling and simulation. *Mech Time-Depend Mater*, 2025;29(1):16.
[54] F. Ahmed *et al.*, "Numerical modeling of a MHD non-linear radiative Maxwell nano fluid with activation energy," *Heliyon*, vol. 10, no. 2, 2024.
[55] Hassan T, Ullah Z, Khan A, Zaman G, Khan I, Alqahtani S. Impact of Activation Energy on Maxwell Nanofluid in a Porous Medium. *BioNanoScience* 2024:1–13.
[56] Syam MM, Morsi F, Eida AA, Syam MI. Investigating convective Darcy–Forchheimer flow in Maxwell Nanofluids through a computational study. *Partial Differ Equ Appl Math*, 2024;11:100863.
[57] Zainodin S, Jamaludin A, Nazar R, Pop I. Impact of heat source on mixed convection hybrid ferrofluid flow across a shrinking inclined plate subject to convective boundary conditions. *Alex Eng J*, 2024;87:662–81.